

Supporting Information

Theoretical study on the reaction of Ti⁺ with acetone and the role of intersystem crossing

Joonghan Kim,¹ Tae Kyu Kim,*² and Hyotcherl Ihee*,¹

¹Center for Time-Resolved Diffraction, Department of Chemistry,
Graduate School of Nanoscience & Technology (WCU), KAIST,
Daejeon, 305-701, Republic of Korea

²Department of Chemistry and Chemistry Institute for Functional Materials,
Pusan National University, Pusan, 609-735, Republic of Korea

* Corresponding author e-mail: ihee57@gmail.com (H. I.) and e-mail: tkkim@pusan.ac.kr (T. K. K.)

Table S1. Bond dissociation energies (ΔH at 298 K) of $\text{Ti}^+(\text{H}_2\text{O})_n$, $\text{Ti}^+(\text{NH}_3)_n$ (n= 1 and 2), and (D_θ at 298 K) $\text{Ti}^+(\text{C}_2\text{H}_4)$ calculated by various DFT functionals with the aug-cc-pVTZ basis set.

| DFT/aug-cc-pVTZ | B3LYP | B3P86 | PBE0 | B98 | M05 | Exp. |
|--|-------|-------|------|------|------|---------------------------|
| $\text{Ti}^+(\text{H}_2\text{O}) \rightarrow \text{Ti}^+ + \text{H}_2\text{O}$ | 37.4 | 38.0 | 37.5 | 35.3 | 33.7 | $37.7 \pm 1.4^{\text{a}}$ |
| $\text{Ti}^+(\text{H}_2\text{O})_2 \rightarrow \text{Ti}^+(\text{H}_2\text{O}) + \text{H}_2\text{O}$ | 32.8 | 33.7 | 33.3 | 31.4 | 28.3 | $32.6 \pm 1.2^{\text{a}}$ |
| $\text{Ti}^+(\text{NH}_3) \rightarrow \text{Ti}^+ + \text{NH}_3$ | 46.7 | 47.7 | 47.3 | 44.6 | 42.4 | $47.1 \pm 1.7^{\text{b}}$ |
| $\text{Ti}^+(\text{NH}_3)_2 \rightarrow \text{Ti}^+(\text{NH}_3) + \text{NH}_3$ | 37.9 | 39.5 | 39.1 | 37.6 | 37.3 | $42.1 \pm 4.1^{\text{b}}$ |
| $\text{Ti}^+(\text{C}_2\text{H}_4) \rightarrow \text{Ti}^+ + \text{C}_2\text{H}_4$ | 30.5 | 35.1 | 34.6 | 34.0 | 34.7 | $34.9 \pm 2.6^{\text{c}}$ |

a: reference¹

b: reference²

c: reference³

Figure S1. Selective molecular orbitals of $^4\text{IM1}$ and $^2\text{IM2}$. Natural electron configurations of Ti, C(2), and O are summarized.

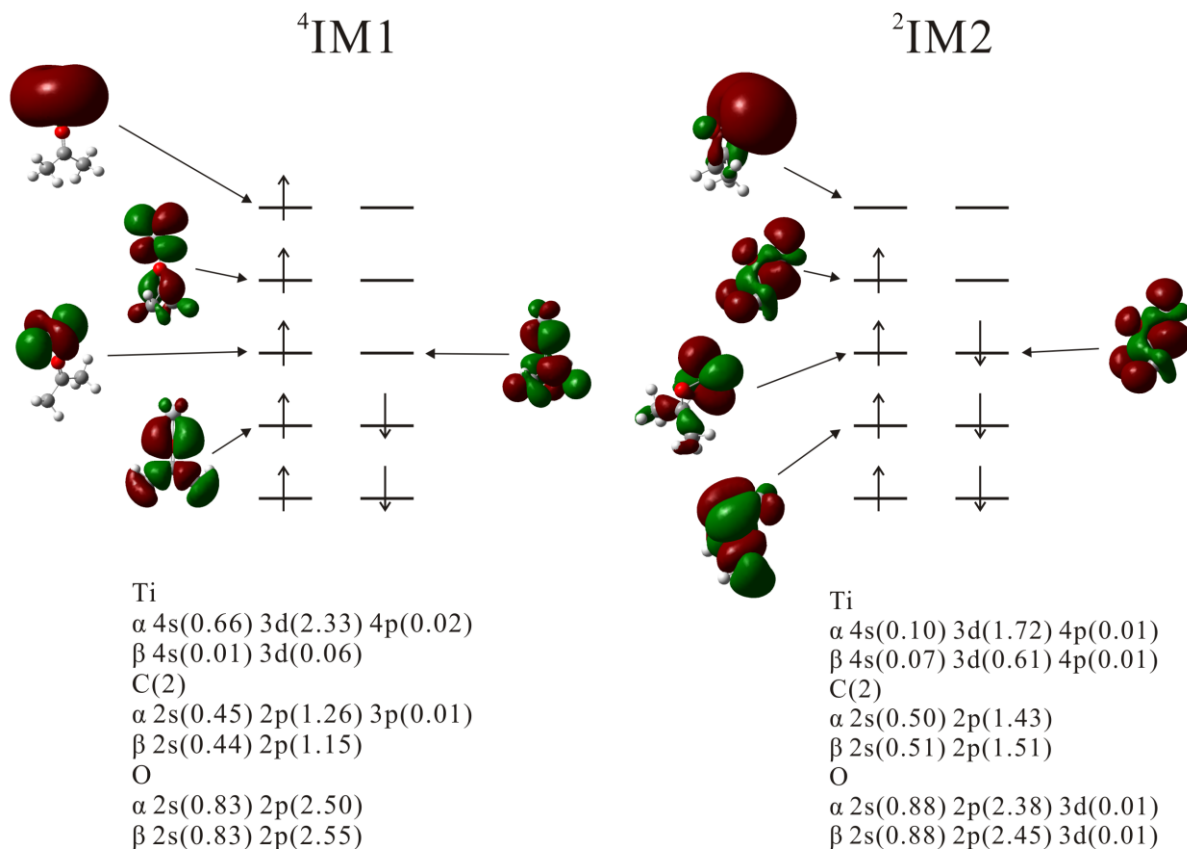


Figure S2. Singly occupied molecular orbital (SOMO) of the $^2\text{IM}4$. It indicates that 3d orbital of Ti interacts with π^* orbital of C=C.

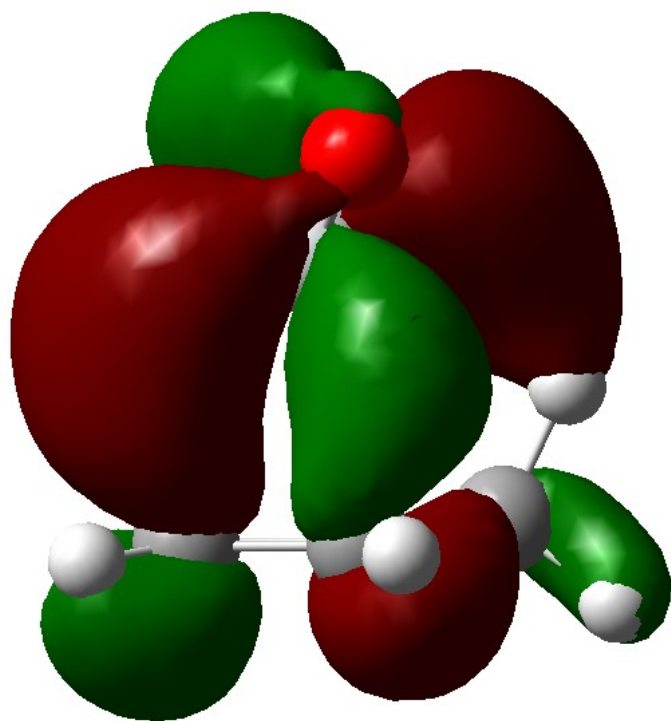


Figure S3. Selected parameters (bond lengths in Å and angles in degree) of optimized geometries calculated by the PBE0/aug-cc-pVTZ on reaction potential energy surfaces of the direct H shift pathway. The superscript denotes the spin multiplicity.

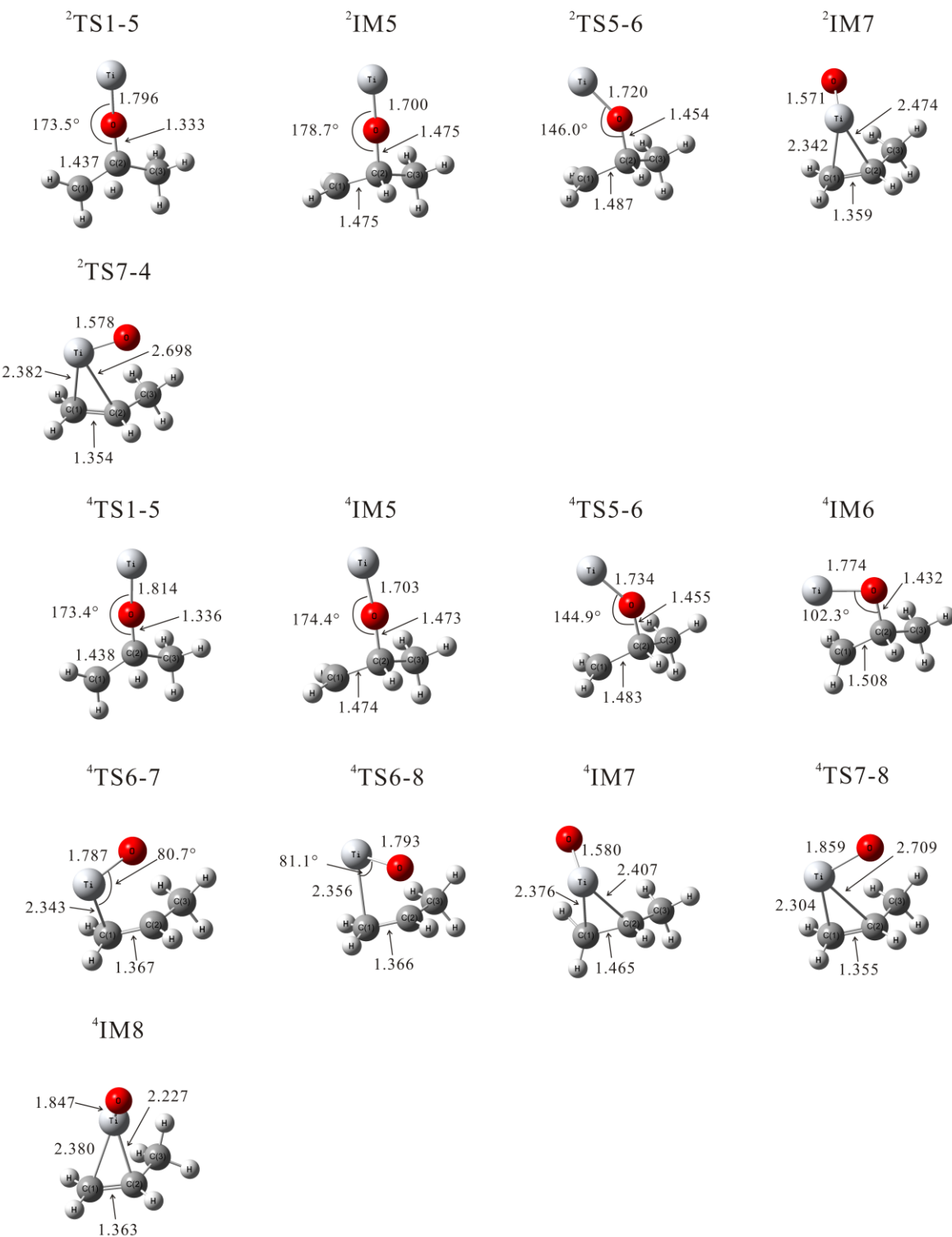


Figure S4. The reaction potential energy surfaces of the direct H shift pathway at the PBE0/aug-cc-pVTZ level. The related optimized structures are depicted in Figure S3 and their energies are summarized in Table S2.

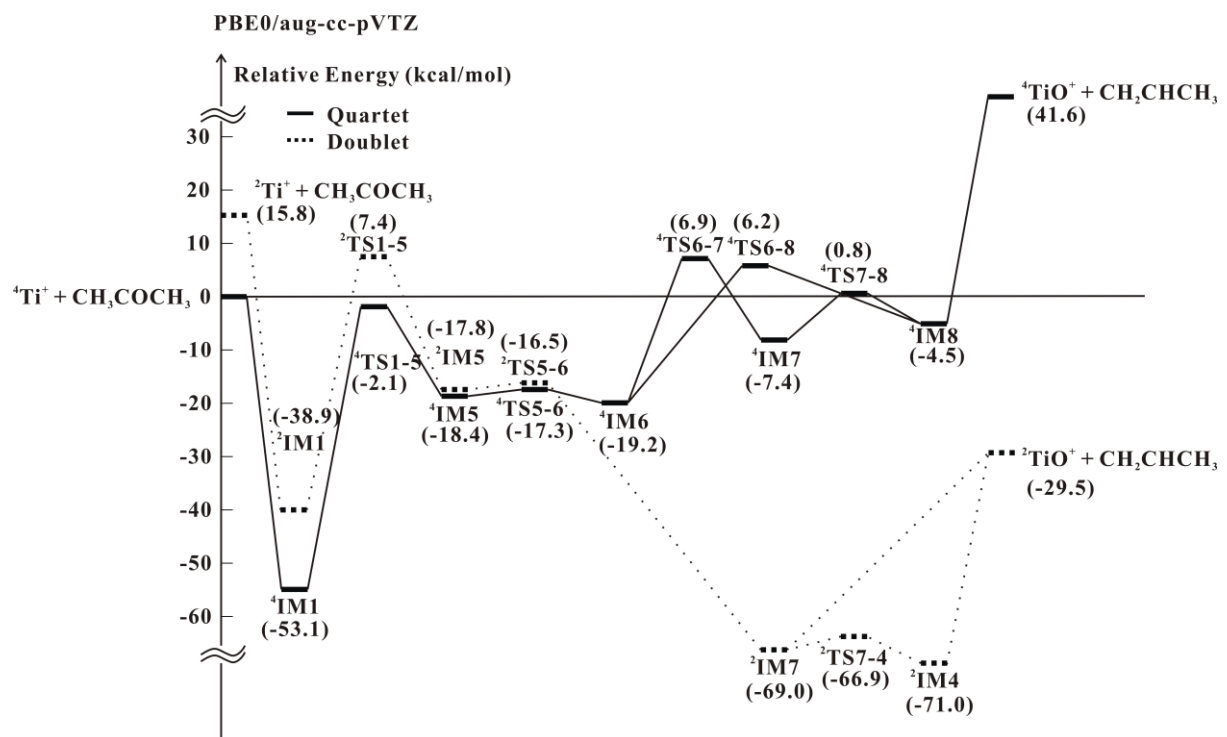


Table S2. Relative energies (ΔE , kcal/mol) calculated by the PBE0/aug-cc-pVTZ, single point relative energies ($\Delta E_{CCSD(T)}$, kcal/mol) calculated by the CCSD(T)/cc-pVTZ, atomic charges (NPA), and $\langle S^2 \rangle$ values for all species involved in the direct H shift pathway.^a

| Doublet | ² TS1-5 | ² IM5 | ² TS5-6 | - | - | - | ² IM7 | ² TS7-4 | ² IM4 |
|-----------------------------|-----------------------|------------------|--------------------|------------------|--------------------|--------------------|------------------|--------------------|------------------|
| ΔE | 7.4(7.6) | -17.8(-17.4) | -16.5(-16.3) | | | | -69.0(-68.5) | -66.9(-66.5) | -71.0(-70.5) |
| $\Delta E_{CCSD(T)}$ | 16.8 | -13.6 | -10.4 | | | | -70.5 | -70.2 | -71.7 |
| Ti | 1.102 | 1.352 | 1.367 | | | | 1.571 | 1.557 | 1.365 |
| O | -0.821 | -0.782 | -0.776 | | | | -0.645 | -0.677 | -0.545 |
| ^b Atomic Charges | C(1) | -0.298 | -0.233 | -0.273 | - | - | -0.554 | -0.660 | -0.455 |
| | C(2) | 0.136 | 0.011 | 0.018 | | | -0.180 | -0.019 | -0.218 |
| | C(3) | -0.633 | -0.622 | -0.621 | | | -0.666 | -0.678 | -0.685 |
| | $\langle S^2 \rangle$ | 1.737 | 1.763 | 1.732 | | | 0.758 | 0.759 | 0.758 |
| Quartet | ⁴ TS1-5 | ⁴ IM5 | ⁴ TS5-6 | ⁴ IM6 | ⁴ TS6-7 | ⁴ TS6-8 | ⁴ IM7 | ⁴ TS7-8 | ⁴ IM8 |
| ΔE | -2.1(-1.9) | -18.4(-18.0) | -17.3(-17.1) | -19.2(-18.9) | 6.9(7.5) | 6.2(6.8) | -7.4(-6.9) | 0.8(1.4) | -4.5(-3.9) |
| $\Delta E_{CCSD(T)}$ | 12.9 | -14.1 | -11.1 | -12.1 | 13.5 | 13.0 | -3.1 | 5.0 | -0.5 |
| Ti | 1.097 | 1.340 | 1.386 | 1.311 | 1.259 | 1.276 | 1.434 | 1.342 | 1.328 |
| ^b Atomic Charges | O | -0.833 | -0.784 | -0.801 | -0.728 | -0.523 | -0.521 | -0.671 | -0.482 |
| | C(1) | -0.221 | -0.222 | -0.253 | -0.343 | -0.548 | -0.533 | -0.379 | -0.675 |
| | C(2) | 0.091 | 0.011 | 0.010 | -0.004 | 0.003 | -0.044 | -0.221 | -0.009 |
| | C(3) | -0.626 | -0.622 | -0.621 | -0.601 | -0.670 | -0.684 | -0.670 | -0.682 |
| $\langle S^2 \rangle$ | 3.796 | 3.767 | 3.766 | 3.763 | 3.769 | 3.770 | 3.765 | 3.756 | 3.756 |

a: values in parenthesis are calculated by the aug-cc-pVQZ.

b: the related figures are depicted in Figure S3.

Figure S5. Selected parameters (bond lengths in Å and angles in degree) of optimized geometries calculated by the PBE0/aug-cc-pVTZ on reaction potential energy surfaces of the metal-mediated H migration pathway. The superscript denotes the spin multiplicity.

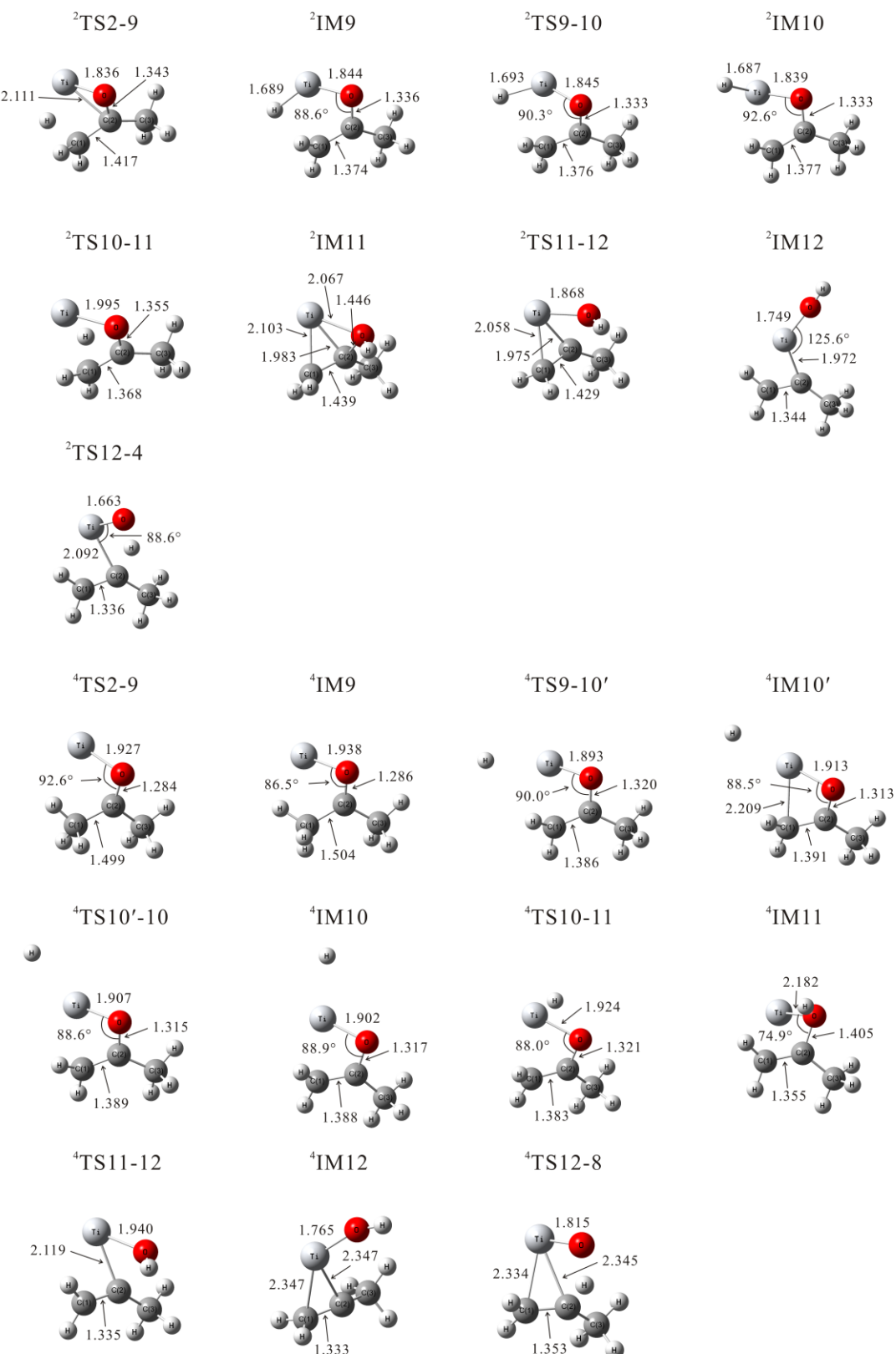


Figure S6. The reaction potential energy surfaces of the metal-mediated H migration pathway at the PBE0/aug-cc-pVTZ level. The related optimized structures are depicted in Figure S5 and their energies are summarized in Table S3.

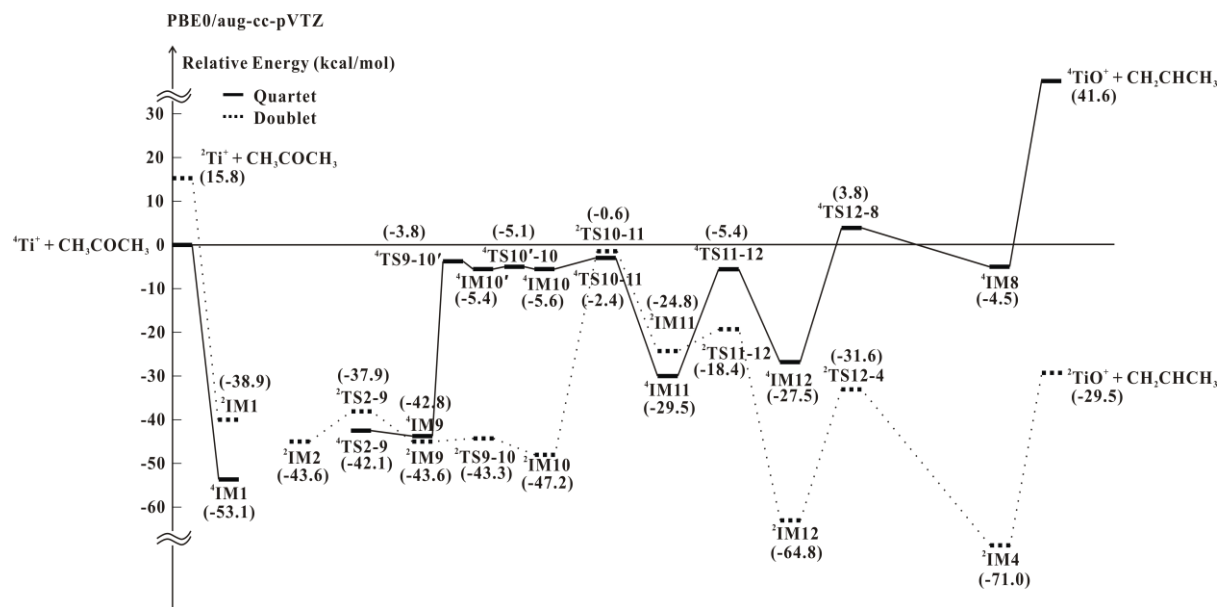


Table S3. Relative energies (ΔE , kcal/mol) calculated by the PBE0/aug-cc-pVTZ, single point relative energies ($\Delta E_{CCSD(T)}$, kcal/mol) calculated by the CCSD(T)/cc-pVTZ, atomic charges (NPA), and $\langle S^2 \rangle$ values for all species involved in the metal-mediated H migration pathway.^a

| Doublet | ² TS2-9 | ² IM9 | ² TS9-10 | - | - | ² IM10 | ² TS10-11 | ² IM11 | ² TS11-12 | ² IM12 | ² TS12-4 |
|-----------------------------|--------------------|------------------|----------------------|--------------------|-----------------------|-------------------|----------------------|-------------------|----------------------|-------------------|---------------------|
| ΔE | -37.9 (-37.6) | -43.6 (-43.3) | -43.3 (-43.0) | | | -47.2 (-47.0) | -0.6 (-0.3) | -24.8 (-24.6) | -18.4 (-18.0) | -64.8 (-64.5) | -31.6 (-31.2) |
| $\Delta E_{CCSD(T)}$ | -30.9 | -39.1 | -39.2 | | | -42.1 | 5.3 | -19.4 | -9.8 | -61.5 | -28.4 |
| Ti | 1.324 | 1.416 | 1.575 | | | 1.560 | 1.108 | 1.349 | 1.389 | 1.631 | 1.456 |
| O | -0.602 | -0.620 | -0.660 | - | - | -0.645 | -0.656 | -0.746 | -0.853 | -0.971 | -0.708 |
| ^b Atomic Charges | C(1) | -0.557 | -0.513 | -0.548 | | -0.651 | -0.654 | -0.756 | -0.814 | -0.472 | -0.663 |
| | C(2) | 0.232 | 0.323 | 0.341 | | 0.407 | 0.380 | 0.103 | 0.160 | -0.243 | -0.236 |
| | C(3) | -0.670 | -0.676 | -0.682 | | -0.683 | -0.674 | -0.658 | -0.704 | -0.673 | -0.438 |
| $\langle S^2 \rangle$ | 0.784 | 0.765 | 0.763 | | | 0.760 | 1.398 | 0.812 | 0.769 | 0.756 | 0.757 |
| Quartet | ⁴ TS2-9 | ⁴ IM9 | ⁴ TS9-10' | ⁴ IM10' | ⁴ TS10'-10 | ⁴ IM10 | ⁴ TS10-11 | ⁴ IM11 | ⁴ TS11-12 | ⁴ IM12 | ⁴ TS12-8 |
| ΔE | -42.1 (-42.0) | -42.8 (-42.6) | -3.8 (-3.5) | -5.4 (-5.1) | -5.1 (-4.9) | -5.6 (-5.4) | -2.4 (-2.2) | -29.5 (-29.3) | -5.4 (-5.0) | -27.5 (-27.2) | 3.8 (4.4) |
| $\Delta E_{CCSD(T)}$ | -30.6 | -30.7 | 1.9 | 0.5 | 1.2 | 0.5 | 4.0 | -21.1 | 4.5 | -18.9 | 13.7 |
| Ti | 1.143 | 1.131 | 1.246 | 1.246 | 1.257 | 1.231 | 1.249 | 0.954 | 1.232 | 1.385 | 1.430 |
| O | -0.679 | -0.646 | -0.681 | -0.678 | -0.678 | -0.674 | -0.676 | -0.728 | -0.886 | -0.986 | -0.714 |
| ^b Atomic Charges | C(1) | -0.718 | -0.697 | -0.709 | -0.713 | -0.705 | -0.698 | -0.683 | -0.563 | -0.536 | -0.677 |
| | C(2) | 0.437 | 0.403 | 0.394 | 0.411 | 0.404 | 0.405 | 0.385 | 0.231 | 0.096 | 0.142 |
| | C(3) | -0.704 | -0.695 | -0.684 | -0.682 | -0.681 | -0.681 | -0.679 | -0.671 | -0.693 | -0.732 |
| $\langle S^2 \rangle$ | 3.756 | 3.756 | 3.758 | 3.758 | 3.758 | 3.756 | 3.758 | 3.754 | 3.759 | 3.762 | 3.763 |

a: values in parenthesis are calculated by the aug-cc-pVQZ.

b: the related figures are depicted in Figure S5.

Figure S7. Selected parameters (bond length in Å and angle in degree) of optimized geometries of intermediates calculated by the PBE0/aug-cc-pVTZ on the C-H activation reaction coordinate.

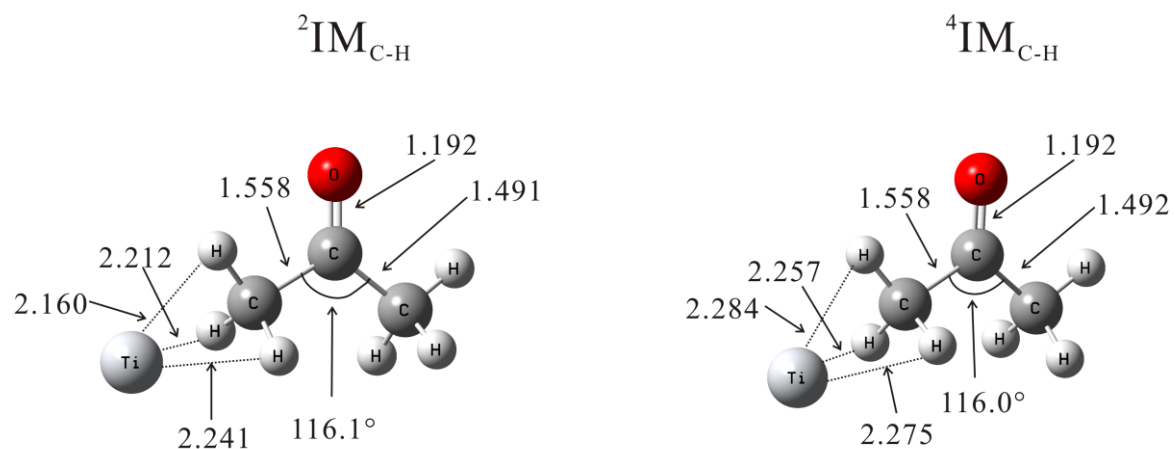
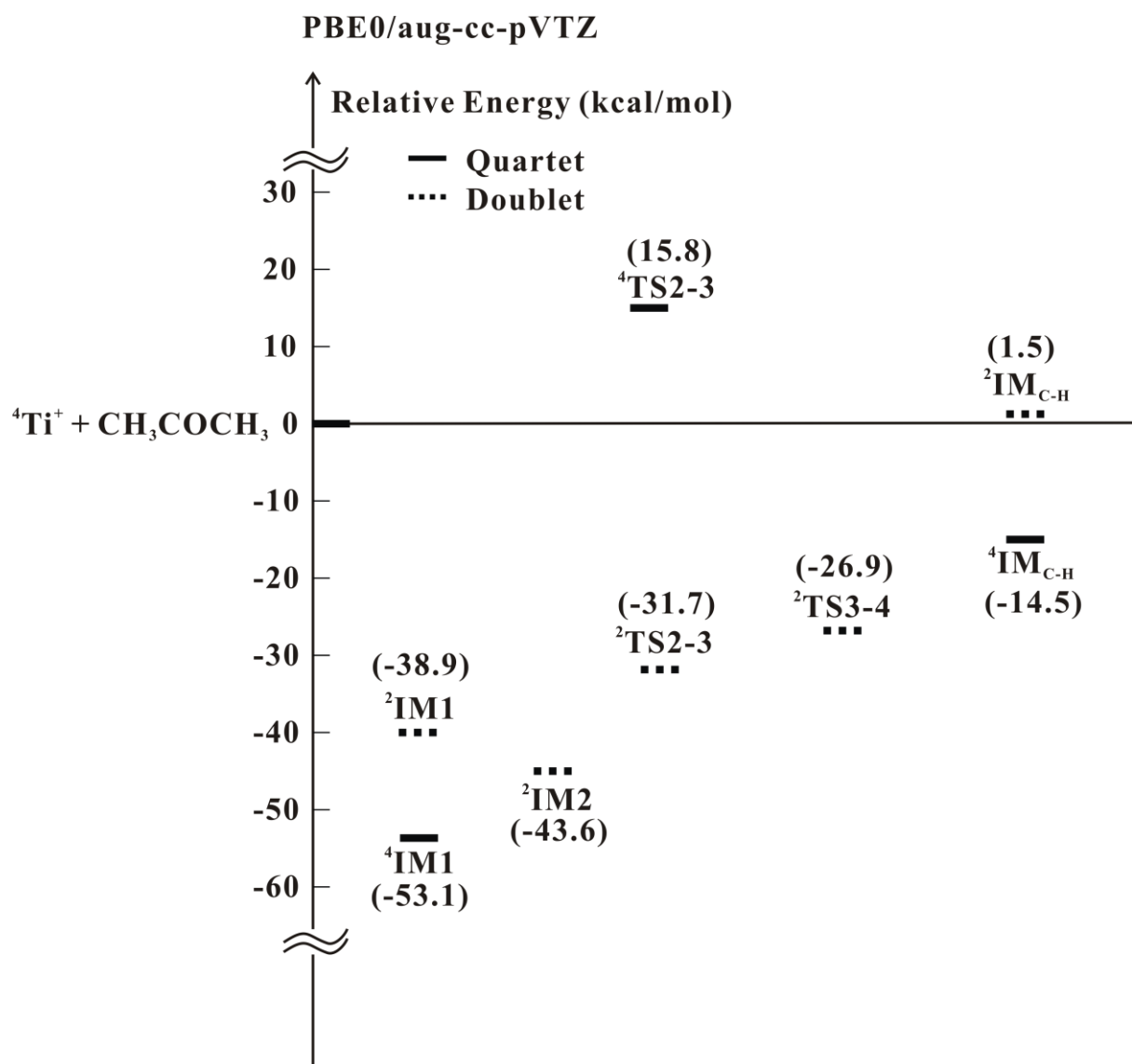


Figure S8. The relative energies of intermediates on the C-H activation reaction coordinate at the PBE0/aug-cc-pVTZ level. The related optimized structures are depicted in Figure S7.



References

- (1) Dalleska, N. F.; Honma, K.; Sunderlin, L. S.; Armentrout, P. B. *J. Am. Chem. Soc.* **1994**, *116*, 3519.
- (2) Walter, D.; Armentrout, P. B. *J. Am. Chem. Soc.* **1998**, *120*, 3176.
- (3) Lide, D. R. *CRC Handbook of Chemistry and Physics*, 88th ed.; CRC Press: Boca Raton, FL, 2008.